Electronic Supplementary Information

B-Embedded Disulfide-Bridged π-Conjugated Compounds: Structures and Optical Tuning

Kaishun Ye,[1] Gang Li,[1,4] Feiyang Li,[1] Chao Shi,[1]* Zhen Jiang,[1] Fuzheng Zhang,[1] Qiuxia Li,[1]* Jie Su,[1] Dandan Song,[2,3]* and Aihua Yuan[1]

[1] School of Environmental and Chemical Engineering, Jiangsu University of Science and Technology, Zhenjiang 212003, P. R. China.

[2] Key Laboratory of Luminescence and Optical Information (Beijing Jiaotong University), Ministry of Education, Beijing 100044, China.

[3] Institute of Optoelectronic Technology, Beijing Jiaotong University, Beijing 100044, China.

[4] CSMC Technologies Fab2 Co., Ltd, Wuxi, 214028, China.

Corresponding Authors' E-mail address

* shichao@just.edu.cn

* liqiuxia2019@just.edu.cn

* ddsong@bjtu.edu.cn

Contents:

General information

Unless noted, all reagents or solvents were obtained from commercial suppliers and used without further purification. All air sensitive experiments were performed in N_2 atmosphere through schlenk technology. The NMR spectra were measured by using a Bruker 400 MHz MHz spectrometer at room temperature. Mass spectra were conducted at Agilent Technologies 5973N (EI). A Hitachi F-4600 fluorescence spectrophotometer was used to measure phosphorescence spectral. An Edinburgh FLS-980 spectrometer was used to determine phosphorescence quantum efficiency and lifetimes of the molecules in solution. The experiments for cyclic voltametric were performed by using three electrode cell assemblies from an IM6ex instrument (Zahner). A one-compartment cell equipped with a platinum wire counter electrode, a Ag/Ag^+ reference electrode, and a glassy-carbon working electrode was used for all measurements with a scan rate of 100 mVs^{-1}. The concentration of tetrabutylammonium hexafluorophosphate (Bu_4NPF_6) in dichloromethane solution was 0.10 $molL^{-1}$ and used as supporting electrolyte.

Synthesis and characterization

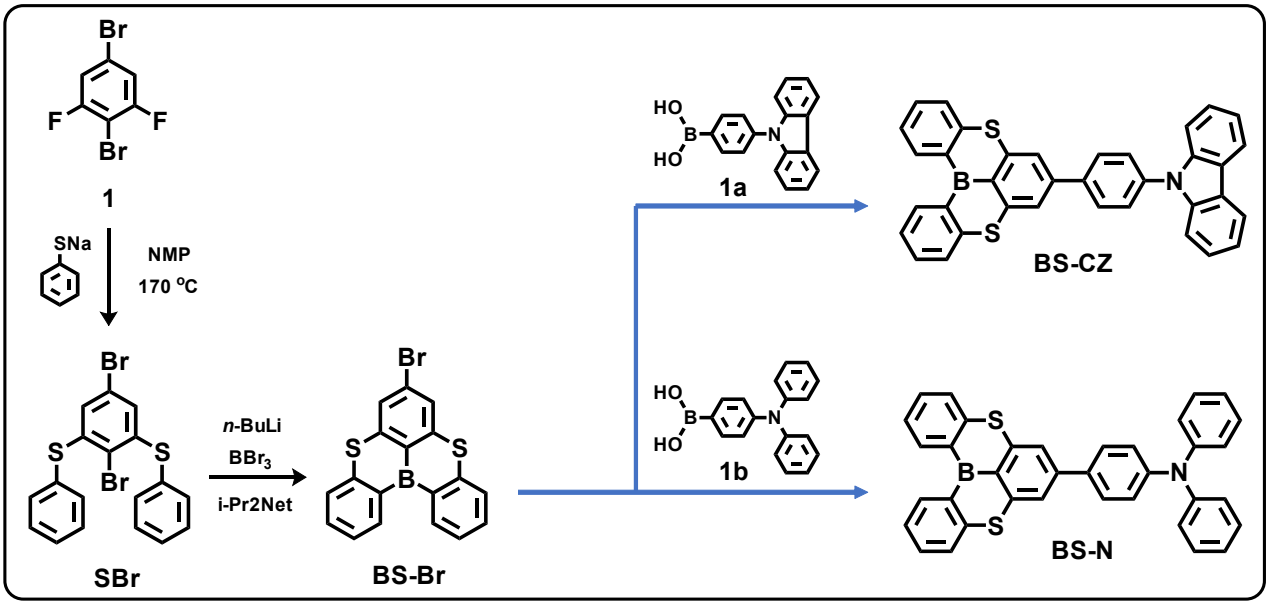

Figure S1. The synthetic routes of B-embedded disulfide-bridged π-conjugated molecules **BS-CZ**, and **BS-N**.

SBr: 2,5-dibromo-1,3-difluorobenzene (5.44 g, 0.02 mol) and sodium benzenethiolate (5.29 g, 0.04 mol) were were added into a double-neck bottle, followed by N-methylpyrrolidone (20 mL) under nitrogen atmosphere. Then the mixture was stirred at 170 °C for 3 h. The reaction mixture was cooled to room temperature, followed by water and extracted with ethyl acetate three times. The combined organic phase was dried and concentrated in vacuum, and target product was purified by column chromatography on silica gel with CH_2Cl_2 / petroleum ether 1 : 6 (v/v) to afford white solid. 6.2 g (65 %). ^{1}H NMR (400 MHz, $CDCl_3$) δ 7.52 (m, 4H), 7.45 (dp, *J* = 4.8, 1.8 Hz, 6H), 6.58 (s, 2H). ^{13}C NMR (101 MHz, $CDCl_3$) δ 143.3, 134.9, 131.4, 130.2, 129.7, 127.1, 122.0, 118.5. $C_{18}H_{12}Br_2S_2$ calcd: C, 47.81; H, 2.67. Found: C, 47.79; H, 2.71. EI-MS (*m/z*): 452.2 (M^+, 100 %).

BS-Br: SBr (1.35 g, 3.0 mmol) was charged to a 100 mL schlenck tube, followed by *m*-xylene (15 mL) under nitrogen atmosphere. *n*-BuLi (1.56 mL, 3.9 mmol) was added at 0 °C, and the resulting mixture was stirred for 20 min at 0 °C. Then, the mixture was warmed up to room temperature and stirred for another 1 h. BBr_3 (0.375 mL, 3.9 mmol) was added at 0 °C and the mixture was stirred for 20 min at 0 °C, then the mixture was warmed up to room temperature and stirred for 50 min. Ethyldiisopropylamine (1.03 mL, 5.84 mmol) was added at 0 °C, then the mixture was heated to 150 °C and stirred for 12 h. The resulting solution was saturated with sodium acetate solution and extracted with CH_2Cl_2 three times. The combined organic phase was dried and concentrated in vacuum to afford white solid, 0.74 g (65 %). ^{1}H NMR (400 MHz, $CDCl_3$) δ 8.30 (dd, *J* = 7.8, 1.5 Hz, 2H), 7.71 (m, 4H), 7.59 (ddd, *J* = 8.0, 7.2, 1.5 Hz, 2H), 7.46 (m, 2H). ^{13}C NMR (101 MHz, $CDCl_3$) δ 145.1, 142.8, 138.7, 131.2, 129.4, 125.6, 125.5, 124.8, 123.8, 115.2. $C_{18}H_{10}BBrS_2$ calcd: C, 56.73; H, 2.64. Found: C, 56.70; H, 2.68. EI-MS (*m/z*): 381.2 (M^+, 100 %).

BS-CZ: BS-Br (0.076 g, 0.2 mmol), 1a (0.069 g，0.24 mmol), tetrakis(triphenylphosphine)palladium (0.0114 g，0.01 mmol) and K_2CO_3 (0.55 g，4 mmol) were added into a schlenck tube, followed by water (2.00 mL) and 1,4-Dioxane (4.00 mL). The mixture was stirred at 100 °C for 24 h under nitrogen atmosphere. The resulting solution was saturated with water and extracted with dichloromethane three times. The combined organic phase was dried and concentrated in vacuum, and target product was purified by column chromatography on silica gel with CH_2Cl_2/petroleum ether 1 : 3 (v / v) to afford yellow solid, 0.075 g (69 %). ^{1}H NMR (400 MHz, $CDCl_3$) δ 8.36 (dd, *J* = 7.7, 1.5 Hz, 2H), 8.17 (dt, *J* = 7.7, 1.0 Hz, 2H), 7.95 (m, 2H), 7.91 (s, 2H), 7.79 (d, *J* = 1.1 Hz, 1H), 7.77 (d, *J* = 1.1 Hz, 1H), 7.73 (d, *J* = 2.1 Hz, 1H), 7.71 (d, *J* = 2.0 Hz, 1H), 7.61 (m, 2H), 7.47 (m, 6H), 7.32 (m, 2H). ^{13}C NMR (101 MHz, $CDCl_3$) δ 144.3, 143.5, 140.8, 139.7, 138.7, 134.6, 131.6, 131.1, 129.1, 127.6, 126.2, 125.7, 125.3, 123.6, 122.9, 120.5, 120.3, 120.0, 110.9, 110.0. $C_{36}H_{22}BNS_2$ calcd: C, 79.56; N, 2.58; H, 4.08. Found: C, 79.53; N, 2.56; H, 4.11. EI-MS (*m/z*): 544.2 ($(M+1)^+$, 100 %).

BS-N: BS-Br (0.152 g，0.4 mmol), 1b (0.172 g，0.6 mmol), Tetrakis(triphenylphosphine)palladium

(0.0228 g，0.02 mmol) and K_2CO_3 (0.55 g，4 mmol) were added into a schlenck tube, followed by water (2.00 mL) and 1,4-Dioxane (4.00 mL). The mixture was stirred at 100 °C for 24 h under nitrogen atmosphere. The resulting solution was saturated with water and extracted with dichloromethane three times. The combined organic phase was dried and concentrated in vacuum, and target product was purified by column chromatography on silica gel with CH_2Cl_2/petroleum ether 1 : 3 (v / v) to afford yellow solid, 0.142 g (65 %). ^{1}H NMR (400 MHz, $CDCl_3$) δ 8.33 (dd, *J* = 7.8, 1.4 Hz, 2H), 7.78 (s, 2H), 7.74 (dd, *J* = 8.2, 1.2 Hz, 2H), 7.67 (td, *J* = 7.3, 1.7 Hz, 4H), 7.44 (td, *J* = 7.6, 1.2 Hz, 2H), 7.30 (m, 4H), 7.16 (m, 6H), 7.08 (m, 2H). ^{13}C NMR (101 MHz, $CDCl_3$) δ 147.5, 144.0, 143.6, 142.5, 138.6, 135.3, 132.8, 130.9, 129.5, 128.3, 125.7, 125.2, 125.0, 123.5, 123.4, 119.4, 116.5, 103.3. $C_{36}H_{24}BNS_2$ calcd: C, 79.26; N, 2.57; H, 4.43. Found: C, 79.23; N, 2.56; H, 4.45. EI-MS (*m/z*): 545.3 (M^+, 100 %).

X-ray crystal structure analysis

Single-crystals of **BS-CZ** and **BS-N** were both obtained by slow solvent evaporation from the saturated mixed solution of CH_2Cl_2 and ethanol. The X-ray diffraction data were collected on a Bruker Smart CCD Apex DUO diffractometer with graphite monochromated Cu Kα radiation (λ = 1.54178 Å) using the ω-2θ scan mode. All crystal datas are deposited in The Cambridge Crystallographic Data Centre (CCDC: 2251377 for **BS-CZ** and 2251378 for **BS-N**).

Table S1. Crystallographic Data for **BS-CZ** and **BS-N**.

Complex	BS-CZ	BS-N
chemical formula	$C_{36}H_{22}BNS_2$	$C_{36}H_{24}BNS_2$
formula weight	543.47	545.49
crystal size (mm)	0.11 × 0.12 × 0.14	0.11 × 0.12 × 0.13
temperature (K)	150	150
radiation	1.54178	1.54178
crystal system	Monoclinic	Triclinic
space group	P21/c	P-1
a(Å)	9.1668(3)	12.1328(6)
b(Å)	13.6407(5)	12.2744(5)
c(Å)	20.9359(7)	19.0272(9)
α(°)	90	103.921(3)
β(°)	90.621(2)	97.005(3)

γ(°)	90	98.421(3)
V(Å^3)	2617.70(16)	2684.0(2)
Z	4	4
ρ($_{calc}$) (g/cm^3)	1.379	1.350
F (000)	1128.0	1136
absorp.coeff. (mm^{-1})	2.048	1.998
θ range (deg)	3.9 to 66.0	2.4 to 66.0
reflns collected	15058 (R_{int} = 0.034)	28738 (R_{int} = 0.042)
indep. reflns	4549	9347
Refns obs.[$I > 2\sigma(I)$]	3654	7385
data/restr/paras	4549/0/361	9347/0/721
GOF	1.03	1.07
R_1/wR_2 [$I > 2\sigma(I)$]	0.0644/0.1586	0.0765/0.2039
R_1/wR_2 (all data)	0.0729/0.1690	0.0872/0.2190
larg peak and hole(e/Å^3)	0.50/–0.19	0.79/–0.32

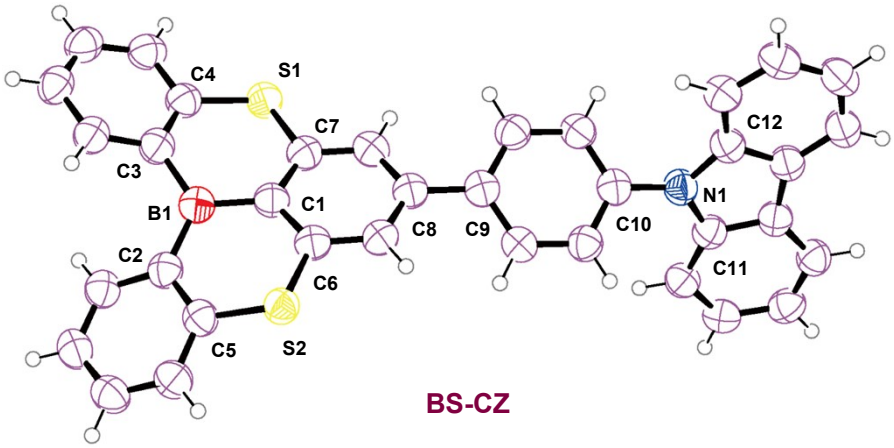

Figure S2. Single crystal structure of **BS-CZ**, selected bond lengths (Å) and angles (°): B1−C1: 1.542(4), B1−C2: 1.547(4), B1−C3: 1.545(4), C8−C9: 1.490(4), N1−C10: 1.427(3), N1−C11: 1.399(3), N1−C12: 1.398(3), S1−C4: 1.759(3), S1−C7: 1.755(3), S2−C5: 1.764(3), S2−C6: 1.756(3), C1–B1–C3: 118.2(2), C1–B1–C2: 118.8(2), C2–B1–C3: 123.0(2), C4–S1–C7: 104.84(12), C5–S2–C6: 105.78(13), C10–N1–C11: 125.9(2), C10–N1–C12: 125.5(2), C11–N1–C12: 108.5(2).

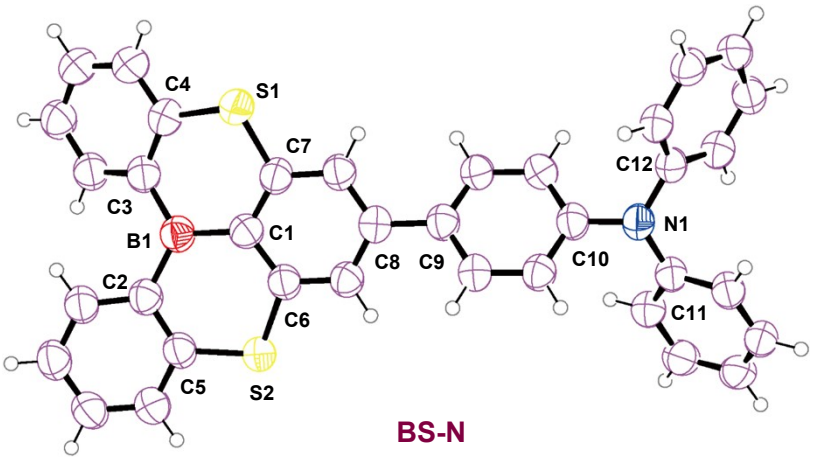

Figure S3. Single crystal structure of **BS-N**, selected bond lengths (Å) and angles (°): B1−C1: 1.551(5), B1−C2: 1.561(5), B1−C3: 1.547(5), C8−C9: 1.489(4), N1−C10: 1.420(4), N1−C11: 1.425(4), N1−C12: 1.429(4), S1−C4: 1.748(4), S1−C7: 1.755(3), S2−C5: 1.751(4), S2−C6: 1.766(3), C1–B1–C3: 118.7(3), C1–B1–C2: 119.2(3), C2–B1–C3: 122.1(3), C4–S1–C7: 106.08(17), C5–S2–C6: 106.11(16), C10–N1–C11: 119.7(2), C10–N1–C12: 119.3(2), C11–N1–C12: 118.6(3).

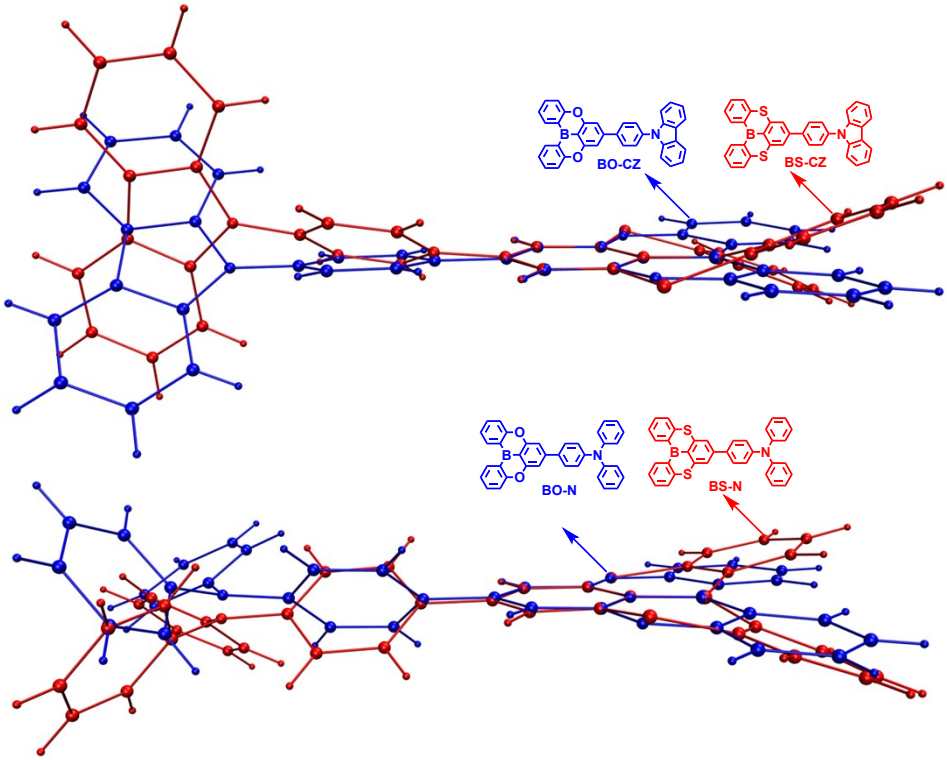

Figure S4. Comparison of single crystal structures of B-embedded disulfide-bridged molecules (**BS-CZ** and **BS-N**) and B-embedded dioxygen-bridged molecules (**BO-CZ** and **BO-N**).

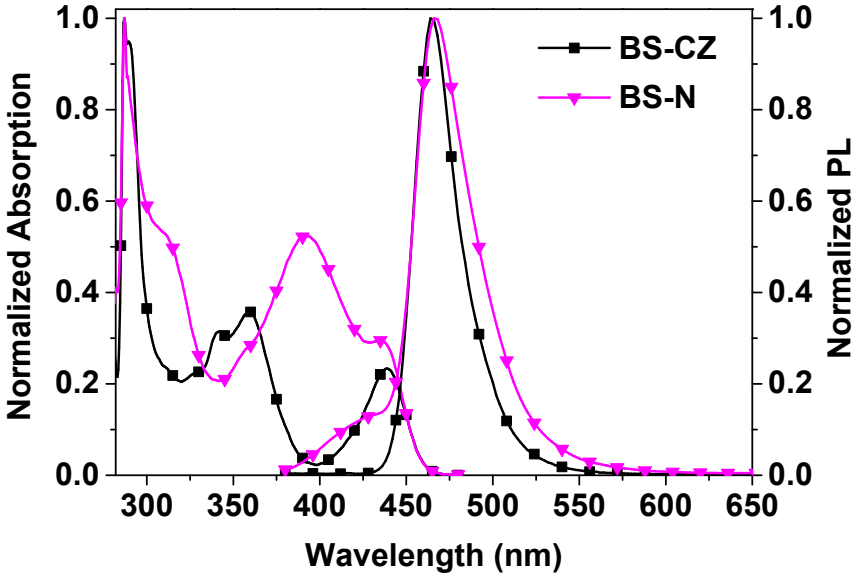

Figure S5. UV-visible absorption spectra and photoluminescence spectra of **BS-CZ** and **BS-N** in toluene (2.0×10^{-5} M) at room temperature.

Solvatochromic PL

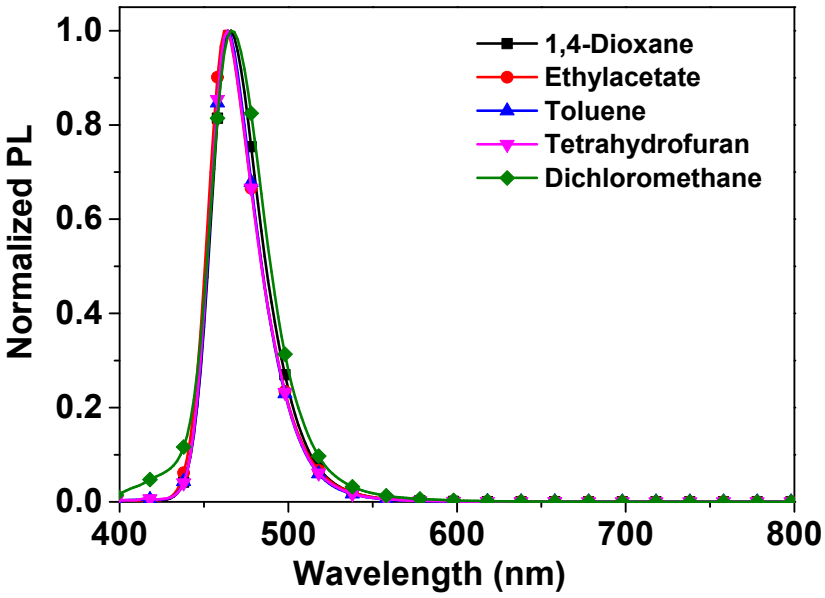

Figure S6. PL spectra of **BS-CZ** in a variety of solvents with different polarities. (Excitation wavelength is 370 nm)

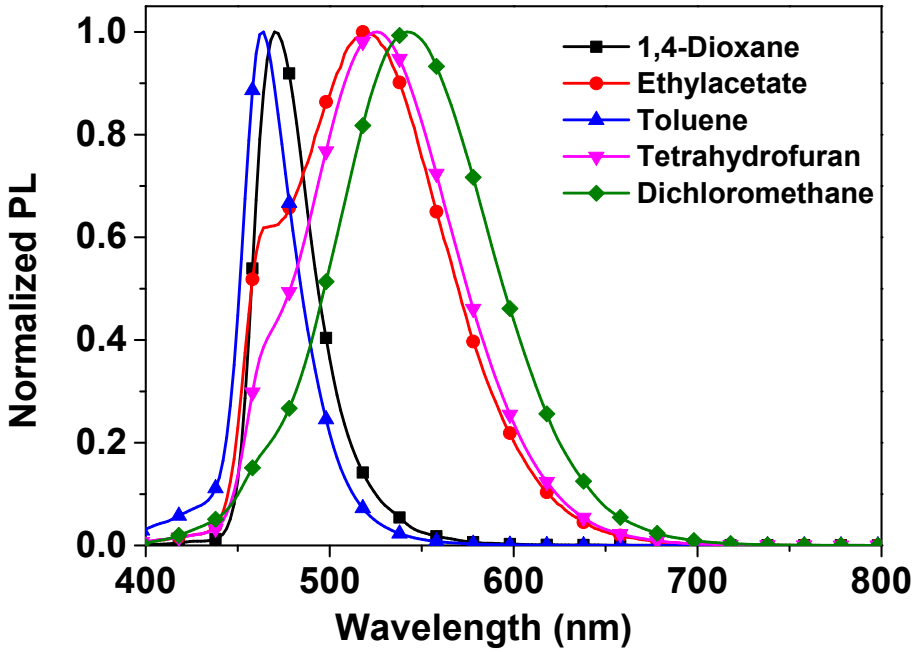

Figure S7. PL spectra of **BS-N** in a variety of solvents with different polarities. (Excitation wavelength is 370 nm)

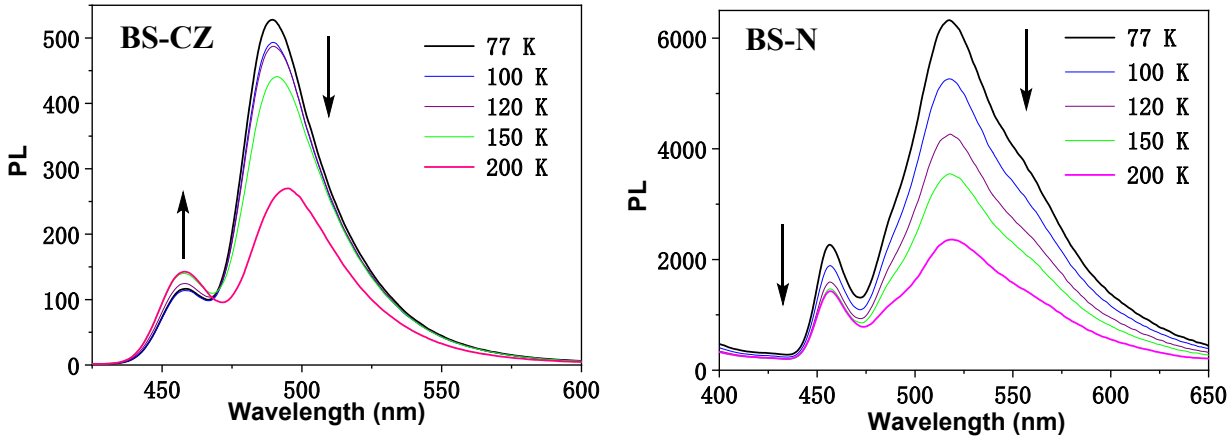

Figure S8. Temperature-dependent PL spectra of **BS-CZ** and **BS-N** in toluene.

TG thermograms

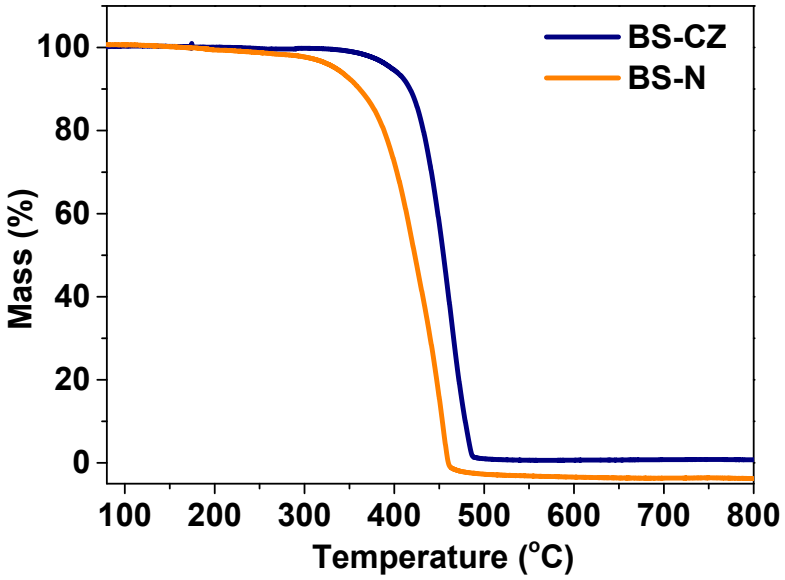

Figure S9. TG thermograms of **BS-CZ** and **BS-N**.

Cyclic voltammetry

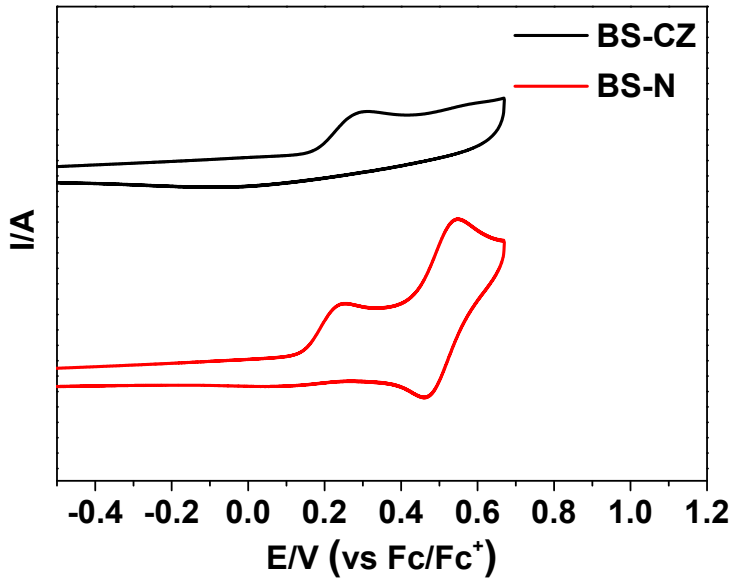

Figure S10. Cyclic voltammogram of **BS-CZ** and **BS-N** in degassed dichloromethane under the scan rate of 100 mV s^{-1}.

DFT calculation

DFT method was used to optimize the geometries all the complexes. The electronic transition energies and electron correlation effects were also calculated by (TD)-DFT method with the B3LYP functional (TD-B3LYP). The 6–31G(d) basis set was used to treat with all atoms. All calculations were carried out according to the Gaussian 09 program.[1] The natural transition orbitals (NTOs) for the transition to singlet and triplet excited states were analyzed by the Multiwfn 3.8 program.[2]

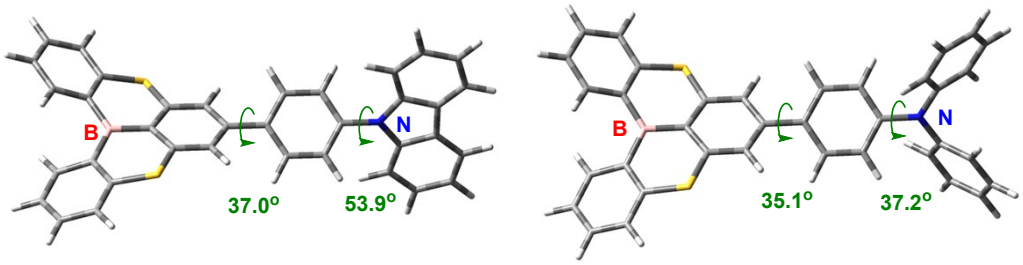

Dipole moment: 2.1704 D
BS-CZ

Dipole moment: 0.7379 D
BS-N

Figure S11. Optimized structures and dipole moment for **BS-CZ** and **BS-N** at the B3LYP/6-31G(d) level of theory.

Table S2. Calculated HOMO, LUMO and E_g of **BS-CZ** and **BS-N**.

Compounds	HOMO (eV)	LUMO (eV)	E_g (eV)
BS-CZ	-5.37	-2.04	3.33
BS-N	-5.03	-1.90	3.14

Table S3. Calculated energies and oscillator strengths of **BS-CZ** and **BS-N** for lowest-energy singlet (S_1) and triplet (T_1) transitions.

Compounds	states	E (eV)	Wavelength (nm)	Oscillator strength	main configurations (CI coeff)
BS-CZ	S_1	2.96	418	0.1077	HOMO-1→LUMO (0.98)
	T_1	2.50	495	0	HOMO-1→LUMO (0.97)
	T_2	2.78	446	0	HOMO→LUMO (0.58)
BS-N	S_1	2.80	443	0.3473	HOMO→LUMO (0.99)
	T_1	2.51	493	0	HOMO-1→LUMO (0.97)
	T_2	2.52	492	0	HOMO→LUMO (0.75)

OLED Device characterization

The ITO coated glass substrates with a sheet resistance of 15 Ω square^{-1} were consecutively ultrasonicated with acetone/ethanol and dried with nitrogen gas flow, followed by 20 min ultraviolet light-ozone (UVO) treatment in a UV-ozone surface processor (PL16 series, Sen Lights Corporation). Then the samples were transferred to the vacuum deposition system, and the organic layers were deposited at the rates of 0.2-3 Å/s sequentially. After the deposition of organic layers, 8-hydroxyquinolinolato-lithium (Liq) as electron injection layer and aluminum (Al) as cathode layer were deposited with rates of 0.1 and 3 Å/s, respectively by thermal evaporation under 5×10^{-5} Pa. The emitting area of the device is about 0.09 cm^2. The current density-voltage-luminance (*J-V-L*), *L-EQE* curves, and electroluminescence spectra were measured using a Keithley 2400 source meter coupled with an absolute EQE measurement system (C9920-12, Hamamatsu Photonics, Japan)

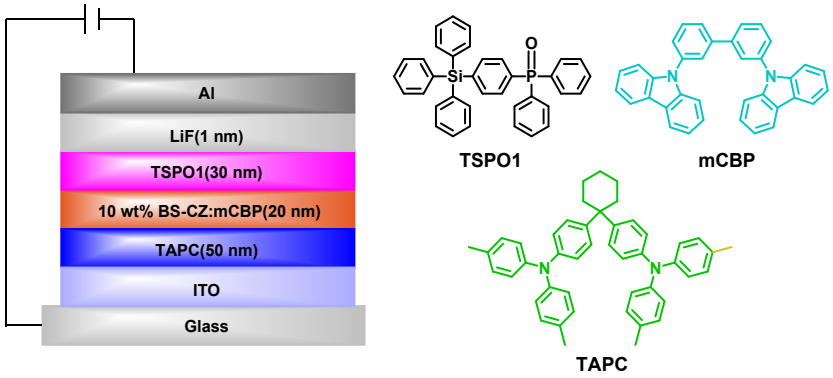

Figure S12. Configuration of the OLED and chemical structures for the materials involved.

Table S4. EL performance of the device for the compound **BS-CZ** and **BS-N**.

Compound	V_{on}[a] (V)	EQE_{max}[b] (%)	λ_{ems}[c] (nm)	FWHM[d] (nm)
BS-CZ	4.0	3.2	473	39
BS-N	4.5	1.6	485	70

[a]Voltage in the luminance of 10 cd/m^2. [b]Maximum external quantum efficiency (EQE_{max}), [c]Maximum emission wavelength of the EL spectra. [d]The full width at half maximum.

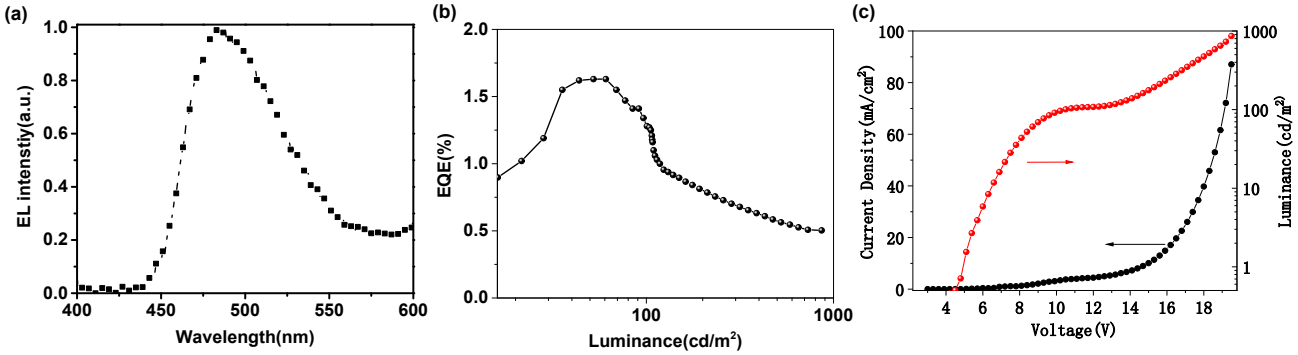

Figure S13. (a) EL spectra, (b) external quantum efficiency (EQE) versus luminance relationship and (c) current density-voltage-luminance (J−V−L) characteristics for the device of **BS-N**.

NMR spectra

^{1}H NMR ($CDCl_3$)

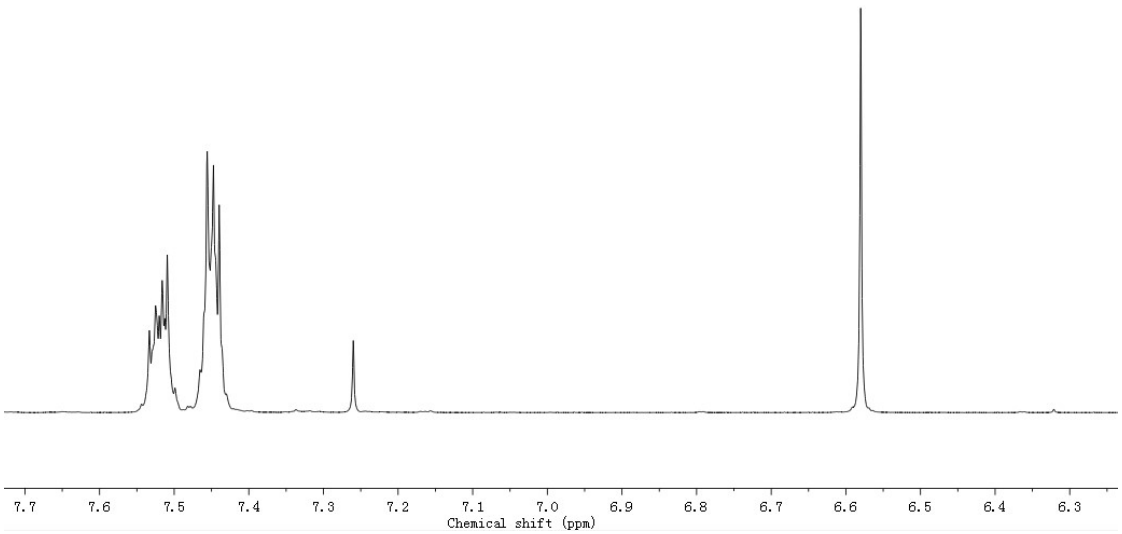

Figure S14. The ^{1}H NMR spectra of **SBr**.

^{13}C NMR ($CDCl_3$)

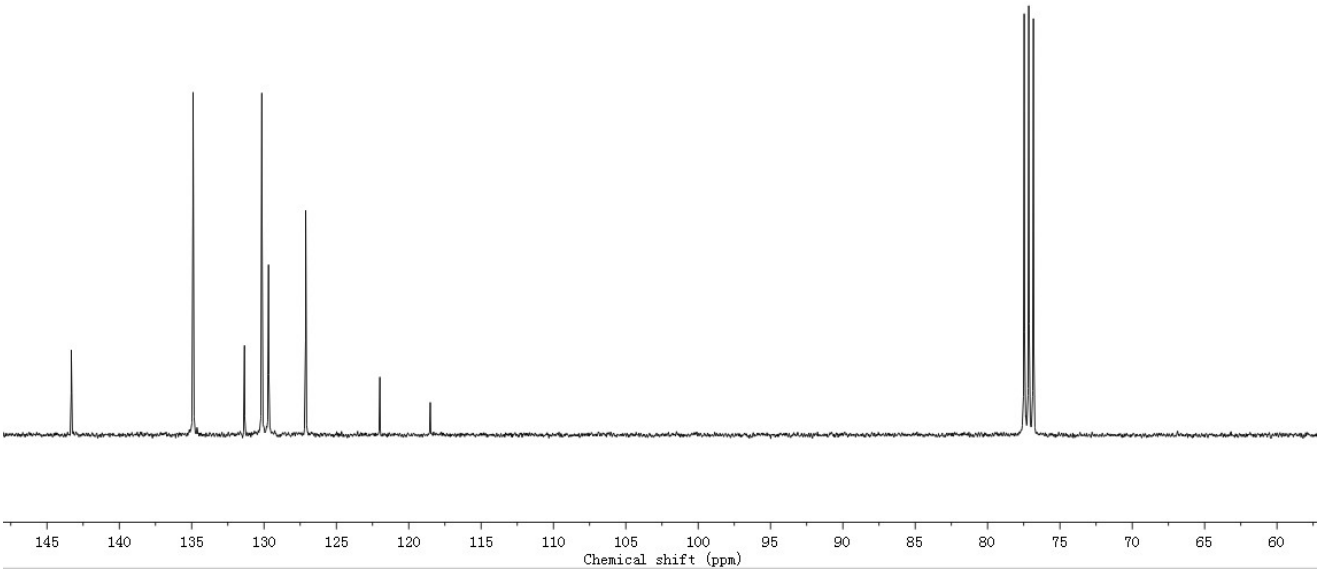

Figure S15. The ^{13}C NMR spectra of **SBr**.

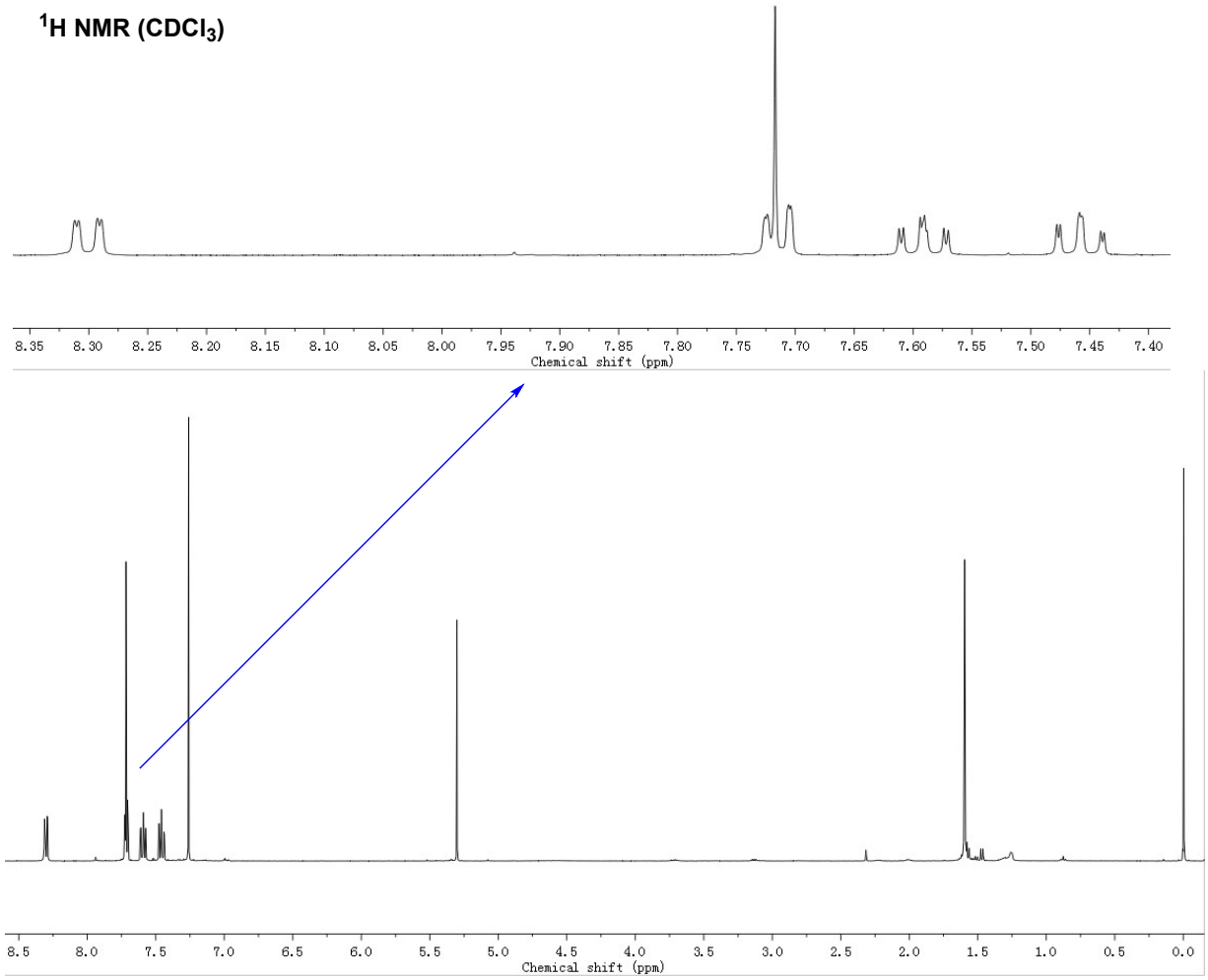

Figure S16. The ^{1}H NMR spectra of **BSBr**.

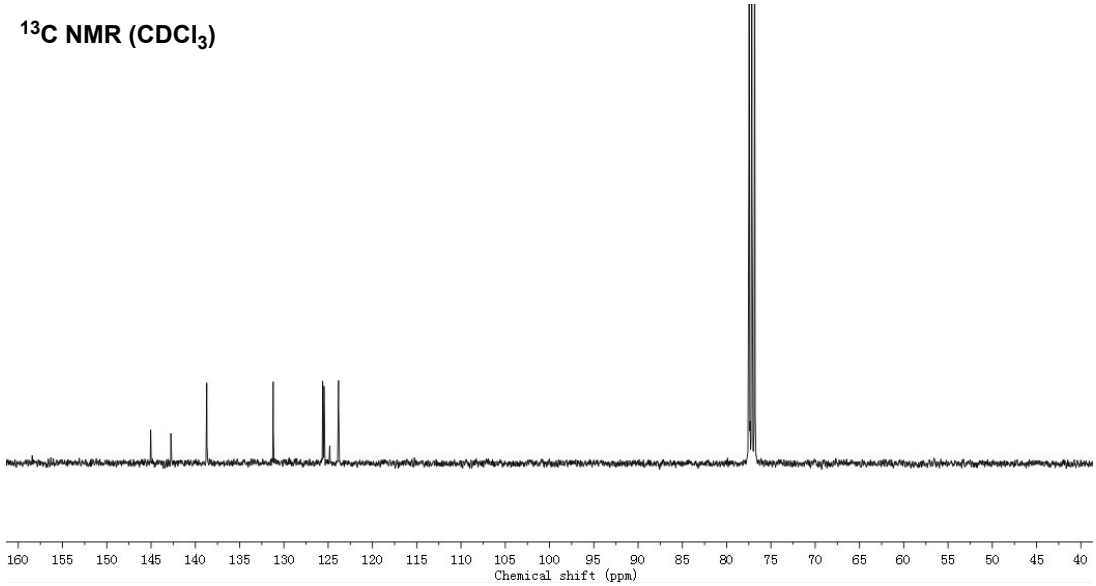

Figure S17. The ^{13}C NMR spectra of **BSBr**.

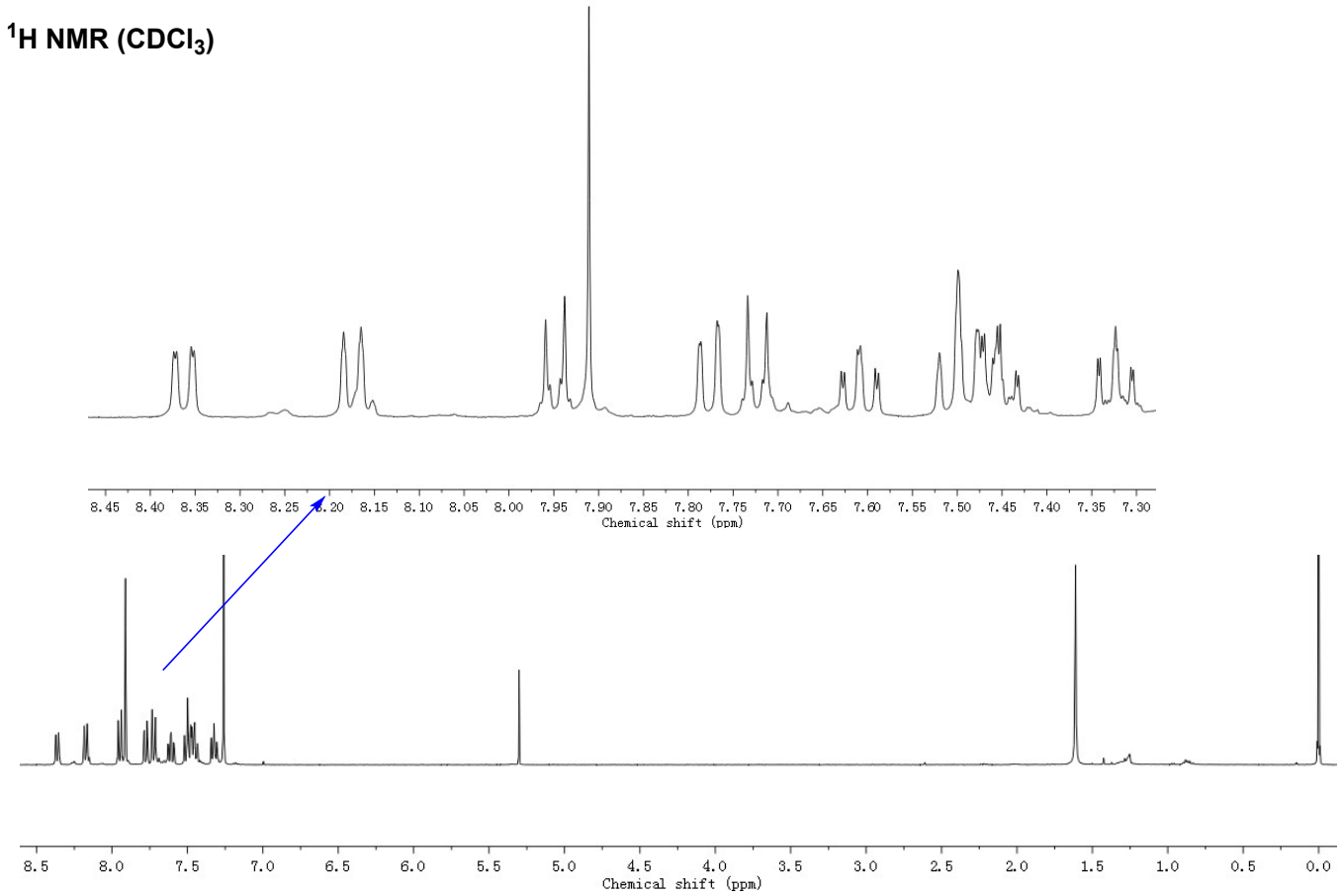

Figure S18. The ^{1}H NMR spectra of **BS-CZ**.

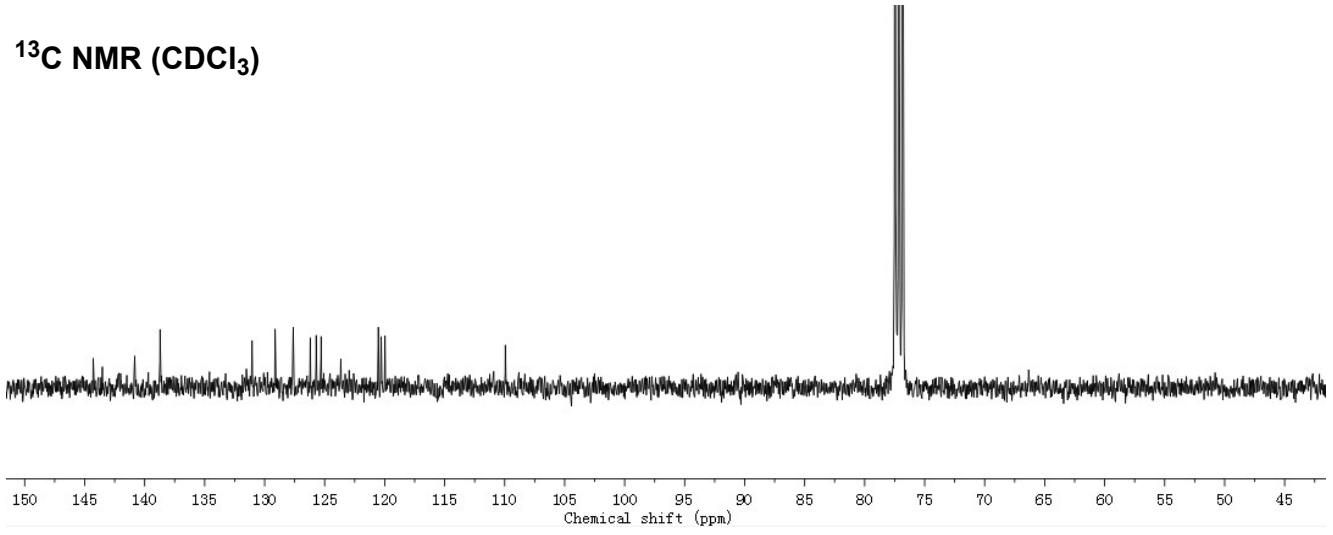

Figure S19. The ^{13}C NMR spectra of **BS-CZ**.

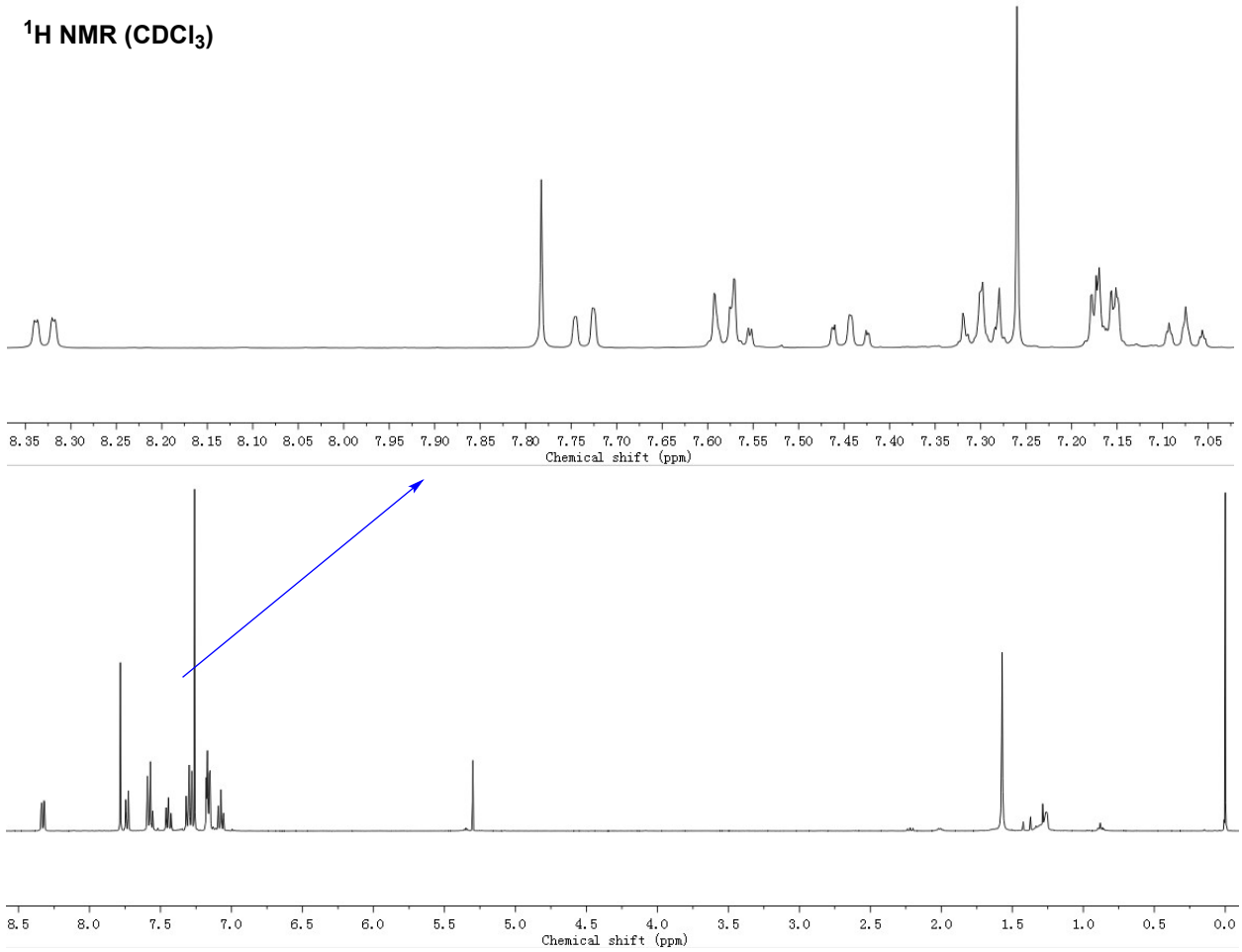

Figure S20. The ^{1}H NMR spectra of **BS-N**.

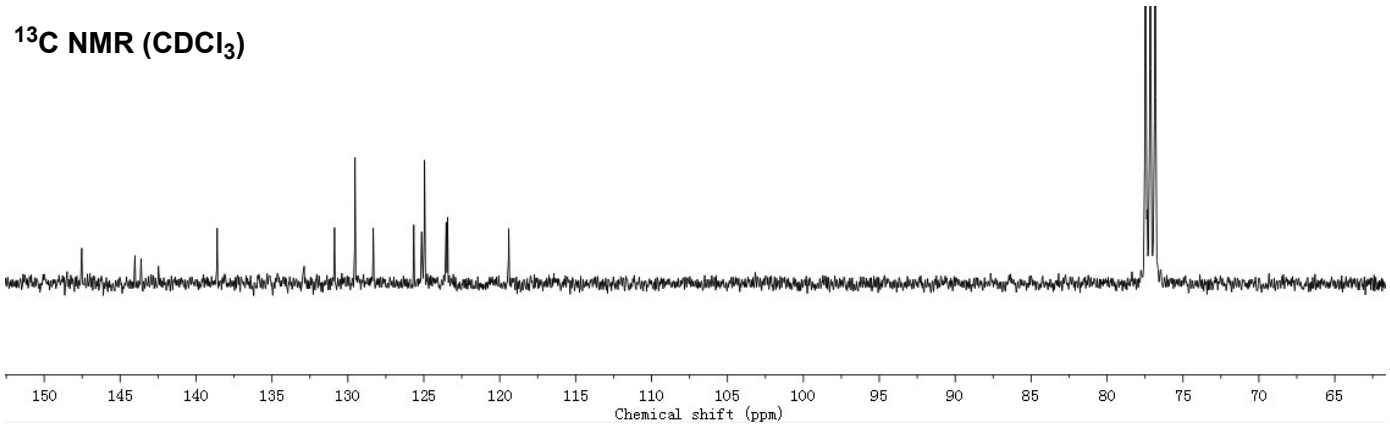

Figure S21. The ^{13}C NMR spectra of **BS-N**.

Mass spectra

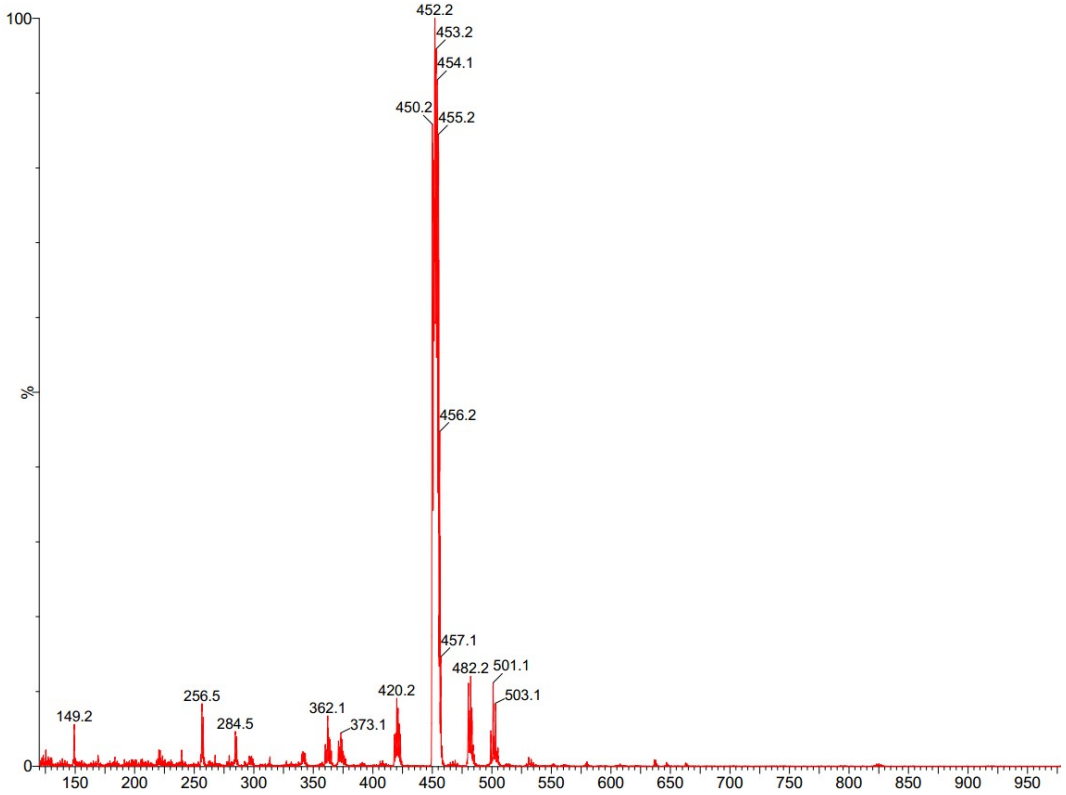

Figure S22. The Mass spectra of **SBr**.

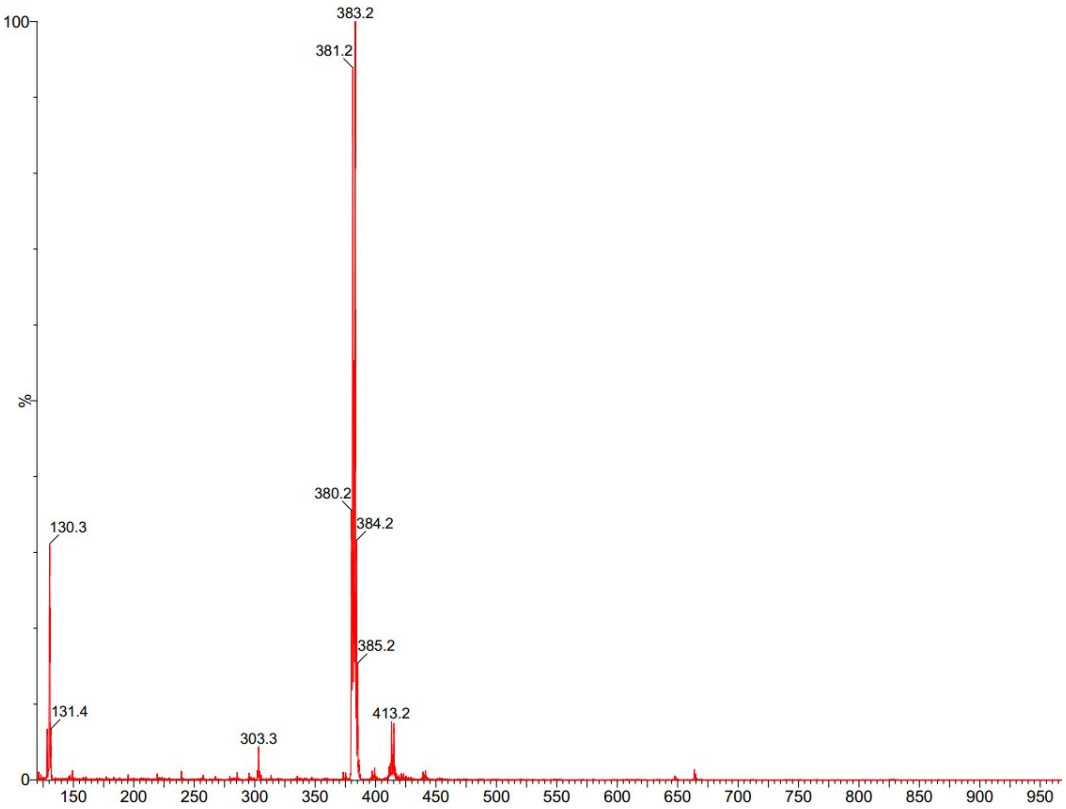

Figure S23. The Mass spectra of **BS-Br**.

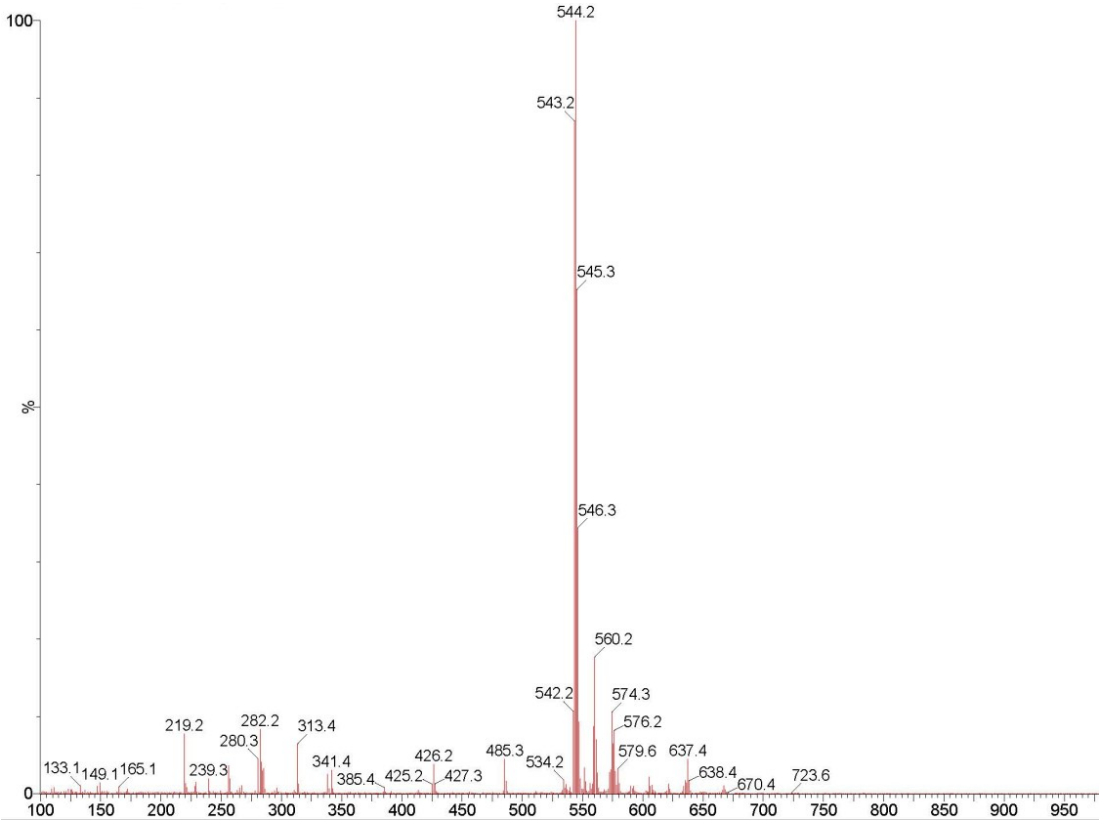

Figure S24. The Mass spectra of **BS-CZ**.

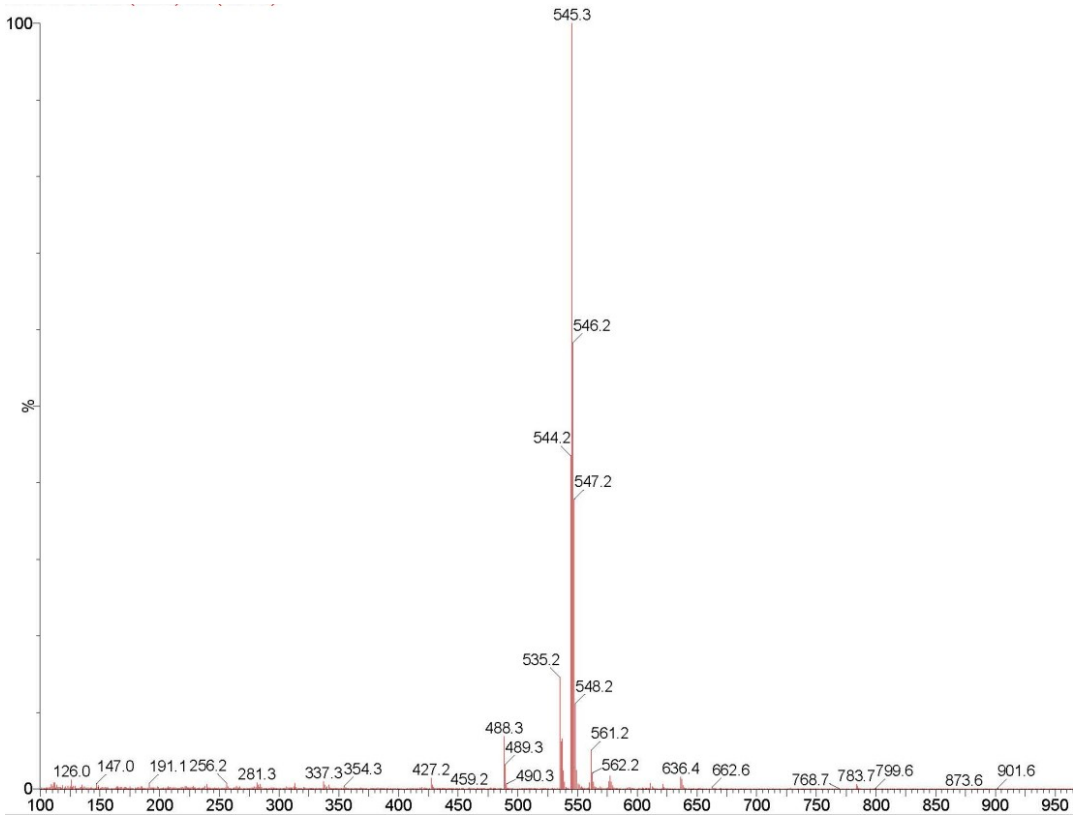

Figure S25. The Mass spectra of **BS-N**.

References

1. M. J. Frisch, G. W. Trucks, H. B. Schlegel, G. E. Scuseria, M. A. Robb, J. R. Cheeseman, G. Scalmani, V. Barone, B. Mennucci, G. A. Petersson, H. Nakatsuji, M. Caricato, X. Li, H. P. Hratchian, A. F. Izmaylov, J. Bloino, G. Zheng, J. L. Sonnenberg, M. Hada, M. Ehara, K. Toyota, R. Fukuda, J. Hasegawa, M. Ishida, T. Nakajima, Y. Honda, O. Kitao, H. Nakai, T. Vreven, J. A. Montgomery Jr., J. E. Peralta, F. Ogliaro, M. Bearpark, J. J. Heyd, E. Brothers, K. N. Kudin, V. N. Staroverov, T. Keith, R. Kobayashi, J. Normand, K. Raghavachari, A. Rendell, J. C. Burant, S. S. Iyengar, J. Tomasi, M. Cossi, N. Rega, J. M. Millam, M. Klene, J. E. Knox, J. B. Cross, V.Bakken, C. Adamo, J. Jaram illo, R. Gomperts, R. E. Stratmann, O. Yazyev, A. J. Austin, R. Cammi, C. Pomelli, J. W. Ochterski, R. L. Martin, K. Morokuma, V. G. Zakrzewski, G. A. Voth, P. Salvador, J. J. Dannenberg, S. Dapprich, A. D. Daniels, O. Farkas, J. B. Foresman, J. V. Ortiz, J. Cioslowski and D. J. Fox, Gaussian 09, Revision B.01, Gaussian, Inc., Wallingford CT, **2010**.
2. T. Lu, F. W. Chen, Multiwfn: A multifunctional wavefunction analyzer. *J. Comput. Chem.* **2012**, *33*, 580.